The closed-form solutions of a diffusive Susceptible-Infectious-Susceptible epidemic model

Rehana Naz [a,*], G. Wang[b], S. Irum[a,**]

July 12, 2024

[a] Department of Mathematics and Statistical Sciences, Lahore School of Economics, Lahore, 53200, Pakistan
[b]School of Mathematics and Statistics, Hebei University of Economics and Business, Shijiazhuang, Hebei, 050061, P.R. China
[*]Corresponding Author Email: nazrehanapk@gmail.com;
[**]Visiting Research Fellow Spring 2022

Abstract

We establish the closed-form solutions of the Susceptible-Infectious-Susceptible (SIS) epidemic model with diffusion using Lie point symmetries. The model admits a four-dimensional Lie algebra. We use different combinations of Lie symmetries to construct the closed-form solutions. We consider appropriate initial and boundary conditions to explore the biological relevance of these closed-form solutions. We utilize the closed-form solutions to study the transmission dynamics of an influenza outbreak with Gaussian initial distributions. We plot graphs for the susceptible and infected populations. We consider the lower diffusion coefficient and higher diffusion coefficient cases to analyze the transmission dynamics of the influenza outbreak.

Keywords

Diffusive SIS model, Lie symmetries, Closed-form Solutions

MSC Classification

22E70, 20C35, 35Q92, 35C05

1 Introduction

Several mathematical models have been developed to study the transitional dynamics of infectious disease. Nonlinear ordinary differential equations (ODEs) and partial differential equations (PDEs) are the powerful

tools for providing a broad perspective of disease persistence or extinction. The ODE epidemic models are based on the assumption that population distribution is homogenous across space. However, the population interaction and distribution are greatly influenced by spatial dispersal, we refer the reader to excellent surveys [1, 2, 3] and reference therein. Noble [4] studied the geographic and temporal development of plagues. The reaction-diffusion equations are utilized to predict the spread of rabies in red fox hosts across Europe [5, 6, 7, 8, 9].

Allen et al [10] developed the SIS epidemic reaction-diffusion models and utilized the Neumann boundary condition to study the effect of spatial heterogeneity of the environment and individual movement on the extinction and persistence of a disease. The rates of disease transmission and recovery were dependent on the location. It was shown that the Disease-Free Equilibrium (DFE) is globally asymptotically stable when the basic reproduction number $\mathcal{R}_0 < 1$ and unstable for $\mathcal{R}_0 > 1$. The existence and uniqueness of Endemic Equilibrium (EE) was guaranteed for $\mathcal{R}_0 > 1$. Moreover, the asymptotic profiles of the EE were determined when the migration rate for susceptible individuals is sufficiently small. Later on, Peng and Liu [11] established global stability of EE for the same diffusion coefficients or by keeping the ratio of disease transmission and recovery rates constant. Allen et al [10] only assessed low and high risk locations, whereas Peng and Liu [11] also included moderate risk areas. Huang et al [12] conducted a subsequent study of a diffusive SIS epidemic model with logistic growth and Dirichlet boundary condition. Later on, Ding et al [13] established the traveling wave solutions linking the DFE and EE for the diffusive SIS epidemic model with constant rates of disease transmission and recovery. We apply the Lie symmetry methods to establish several closed-form solutions of the diffusive SIS epidemic model. Ding et al. [13] proposed the following SIS model:

$$\begin{aligned} S_t &= \delta S_{xx} - \Omega(S,I)I, \\ I_t &= \delta I_{xx} + \Omega(S,I)I, \end{aligned} \tag{1}$$

where $\Omega(S,I) = \frac{\beta S - \gamma(S+I)}{S+I}$. Here $S(t,x)$ denotes the density of susceptible individuals, $I(t,x)$ denotes the density of infected individuals, $\beta > 0$ denotes the infection rate, $\gamma > 0$ is the recovery rate and δ is diffusion coefficient. The total population $N(t,x) = S(t,x) + I(t,x)$ satisfies $N_t = \delta N_{xx}$. Our focus is on addressing the following questions: Does a closed-form solution exist for the diffusive SIS model governed by two nonlinear PDEs? How do varying rates of diffusion both higher and lower impact the spatiotemporal dynamics of influenza transmission? Moreover, we examine how this insight can contribute to the development of effective strategies to control and mitigate the spread of the disease.

The Lie group techniques are effective instruments for methodically constructing closed-form solutions to the differential equations arising in different fields of applied Mathematics. We refer the reader to excellent books [14, 15, 16, 17] on the classical Lie symmetry method and elegant softwares for computation of symmetries [18, 19, 20, 21, 22]. Hereman [23] carried out a comprehensive review of symbolic software developed for Lie symmetry analysis. The symmetry methods are successfully applied to

derive Lie symmetries, first integrals and exact solutions for the epidemic models (see [24, 25]. In [26], the closed-form solutions were utilized to analyze the transmission dynamics of COVID-19 and policies to contain the virus were provided.

This paper is organised as follows: For the diffusive SIS model, we explore the Lie symmetries, closed-form solutions, and reductions in Section 2. We manage to reduce the given system of two second-order PDEs to a more manageable system of two second-order ODEs by starting with the most general Lie symmetry generator. We construct closed-form solutions for two distinct scenarios using a combination of three Lie symmetries. In Section 3, a connection is established between the closed-form solution derived in section 2 for one of scenarios and a real-world scenario to understand the transmission dynamics of influenza. The appropriate initial conditions and boundary conditions are employed. The effect of varying rates of diffusion both higher and lower on the spatiotemporal dynamics of influenza transmission is addressed. Moreover, the development of effective strategies to control and mitigate the spread of the disease are provided. Finally, the concluding remarks are provided in Section 4.

2 Lie symmetries, reductions and Closed-form solutions of SIS epidemic model

Our focus in this section is to addressing the following questions: Does a closed-form solution exist for the diffusive SIS model governed by two nonlinear PDEs? We utilize computer package SADE [22] to establish Lie symmetries of the diffusive SIS model. Then, Lie symmetries are employed to identify reductions and obtain closed-form solutions for the diffusive SIS model. By applying Lie symmetry transformations, we can simplify the system of PDEs governing the model into a more manageable system of ODEs. We explore three scenarios: first, the most general Lie symmetry generator; second, the combination of three symmetries; and third, the combination of two symmetries. The most general Lie symmetry generator results in the reduction of the system of two PDEs to a system of two second-order ODEs, which cannot be solved for closed-form solutions. However, the two more combinations of Lie symmetries are utilized to reduce the system of PDEs (1) to a system of two first-order ODEs. It was possible to find the closed-form solutions of the reduced system of ODEs, thus providing us with the closed-form solution of the original system of PDEs.

The Lie symmetries of system (1) are

$$\begin{aligned} X_1 &= \partial_t, \\ X_2 &= \partial_x, \\ X_3 &= S\partial_S + I\partial_I, \\ X_4 &= 2\delta t\partial_x - xS\partial_S - xI\partial_I. \end{aligned} \tag{2}$$

One can use any computer package [18, 19, 20, 21, 22] to find these Lie symmetries.

2.1 Reductions using Lie symmetries X_1, X_2, X_3 and X_4

The most general symmetry infinitesimal generator is

$$X = c_1\partial_x + c_2\partial_t + c_3(S\partial_S + I\partial_I) + c_4(2\delta t\partial_x - xS\partial_S - xI\partial_I). \tag{3}$$

Now, from the invariance surface conditions, [14, 15, 16, 17], we have

$$(c_1 + 2c_4\delta t)S_x + c_2S_t = (c_3 - c_4x)S, \tag{4}$$

$$(c_1 + 2c_4\delta t)I_x + c_2I_t = (c_3 - c_4x)I. \tag{5}$$

Equations (4) and (5) for $c_1 \neq 0$, yield the group invariant solution of system (1) as

$$\begin{aligned} S(t,x) &= F_1(\xi)e^{\frac{t(4c_4^2\delta t^2 - 6c_1c_4x + 3c_2c_4t + 6c_1c_3)}{6c_1^2}}, \\ I(t,x) &= F_2(\xi)e^{\frac{t(4c_4^2\delta t^2 - 6c_1c_4x + 3c_2c_4t + 6c_1c_3)}{6c_1^2}}, \\ \xi &= \frac{c_1x - c_2t - c_4\delta t^2}{c_1}. \end{aligned} \tag{6}$$

The system of PDEs (1) reduces to the following system of ODEs:

$$\begin{aligned} c_1\delta(F_1+F_2)F_1'' + c_2(F_1+F_2)F_1' - (c_3 - c_4\xi)F_1^2 + c_1\gamma F_2^2 \\ +(c_1\gamma - c_1\beta + c_4\xi - c_3)F_1F_2 = 0, \\ c_1\delta(F_1+F_2)F_2'' + c_2(F_1+F_2)F_2' - (c_1\gamma - c_4\xi + c_3)F_2^2 \\ -(c_1\gamma - c_1\beta - c_4\xi + c_3)F_1F_2 = 0, \end{aligned} \tag{7}$$

provided $c_1 \neq 0$. One can utilize any mathematical software to obtain numerical solutions for system (7). However, it is important to note that our current focus is not on constructing numerical solutions. Our primary focus lies in the derivation of closed-form solutions. This involves considering different combinations of Lie symmetries to obtain closed-form solutions for the system of PDEs (1).

It is important to mention here that we can obtain several reductions of diffusive SIS model (1) by setting one, two, or three of the constants c_2, c_3, c_4 to zero while keeping $c_1 \neq 0$ in the system of reduced second-order ODEs (7). Each combination of Lie symmetries corresponds to a distinct reduction. For example, when we set $c_2 = 0$ in the system of the reduced second-order ODEs (7), this corresponds to the reduction via X_1, X_3, and X_4. By making such adjustments to the constants, we can explore various reduction possibilities for the original system of two second-order PDEs (1) representing the diffusive SIS model.

Next, we explore the possibility of closed-form solutions using different combinations of Lie symmetries X_2, X_3 and X_4.

2.2 The closed-from solution using Lie symmetries X_2, X_3 and X_4

We set $c_1 = 0$ in the most general symmetry infinitesimal generator (3), which is equivalent to considering the combination of Lie symmetries X_2, X_3, and X_4. Then the group invariant solution of system (1) is given by

$$\begin{aligned} S(t,x) &= F_1(t)e^{-\frac{(c_3-c_4x)^2-c_3^2}{2c_4(2c_4\delta t+c_2)}}, \\ I(t,x) &= F_2(t)e^{-\frac{(c_3-c_4x)^2-c_3^2}{2c_4(2c_4\delta t+c_2)}}. \end{aligned} \tag{8}$$

The system of PDEs (1) reduces to the following system of ODEs

$$\begin{aligned} 4\left(c_4\delta t+\frac{1}{2}c_2\right)^2(F_1+F_2)F_1' + \left(2c_4^2\delta^2 t + c_2c_4\delta - c_3^2\delta\right)F_1^2 \\ -4\gamma\left(c_4\delta t+\frac{1}{2}c_2\right)^2F_2^2 - 4\left[\left(\gamma t-\beta t-\frac{1}{2}\right)c_4^2\delta^2 t \\ +\left(\gamma t-\beta t-\frac{1}{4}\right)c_2c_4\delta + \frac{1}{4}c_3^2\delta + \frac{1}{4}c_2^2(\gamma-\beta)\right]F_1F_2 = 0, \\ \left(c_4\delta t+\frac{1}{2}c_2\right)^2(F_1+F_2)F_2' + \left[\left(\gamma t+\frac{1}{2}\right)c_4^2\delta^2 t \\ +\left(\gamma t+\frac{1}{4}\right)c_2c_4\delta - \frac{1}{4}c_3^2\delta + \frac{1}{4}\gamma c_2^2\right]F_2^2 + \left[\left(\gamma t-\beta t+\frac{1}{2}\right)c_4^2\delta^2 t \\ +\left(\gamma t-\beta t+\frac{1}{4}\right)c_2c_4\delta - \frac{1}{4}c_3^2\delta + \frac{1}{4}c_2^2(\gamma-\beta)\right]F_1F_2 = 0. \end{aligned} \tag{9}$$

The solution of reduced system of ODEs (9) is

$$\begin{aligned} F_1(t) &= \frac{\left(e^{-(\beta-\gamma)t}A_1\beta - A_2\gamma\right)e^{-\frac{c_3^2}{2c_4(2c_4\delta t+c_2)}}}{\sqrt{2c_4\delta t+c_2}\,(e^{-(\beta-\gamma)t}A_1-A_2)A_2}, \\ F_2(t) &= \frac{e^{\frac{-c_3^2}{2c_4(2c_4\delta t+c_2)}}(\gamma-\beta)}{\sqrt{2c_4\delta t+c_2}\,(e^{-(\beta-\gamma)t}A_1-A_2)}, \end{aligned} \tag{10}$$

provided $c_4 \neq 0$. Here A_1 and A_2 are arbitrary constants of integration. Substituting the expressions for $F_1(t)$ and $F_2(t)$ from (10) into equation (8), the form of the final group invariant solution of system (1), using a combination of Lie symmetries X_2 , X_3 and X_4 with $c_4 \neq 0$, is as follows:

$$\begin{aligned} S(t,x) &= \frac{e^{-\frac{(c_3-c_4x)^2}{2c_4(2c_4\delta t+c_2)}}\left(e^{-(\beta-\gamma)t}A_1\beta - A_2\gamma\right)}{\sqrt{2c_4\delta t+c_2}\,\left(e^{-(\beta-\gamma)t}A_1-A_2\right)A_2}, \\ I(t,x) &= \frac{e^{-\frac{(c_3-c_4x)^2}{2c_4(2c_4\delta t+c_2)}}(\gamma-\beta)}{\sqrt{2c_4\delta t+c_2}\,\left(e^{-(\beta-\gamma)t}A_1-A_2\right)}. \end{aligned} \tag{11}$$

It is important to mention that the closed-form solution of the diffusive SIS system (1), as provided in equation (11), serves as the benchmark

for deducing closed-form solutions through various combinations of Lie symmetries X_2, X_3, and X_4. Specifically, it corresponds to the closed-form solution obtained via the Lie symmetry X_4 when both c_2 and c_3 are set to zero. Furthermore, this closed-form solution represents the solution resulting from the combination of the Lie symmetries X_2 and X_4 when c_3 is set to zero. Additionally, when c_2 is set to zero, it corresponds to the closed-form solution involving the combination of Lie symmetries X_3 and X_4.

2.3 The closed-form solution using symmetries X_2 and X_3

We set $c_1 = 0$ and $c_4 = 0$ in the most general symmetry infinitesimal generator (3) , which is equivalent to considering the combination of Lie symmetries X_2 and X_3. Then the group invariant solution of system (1) is given by

$$\begin{aligned} S(t,x) &= F_1(t)e^{\frac{c_3}{c_2}x}, \\ I(t,x) &= F_2(t)e^{\frac{c_3}{c_2}x}, \end{aligned} \tag{12}$$

where $c_2 \neq 0$. The system of PDEs (1) reduces to the following system of ODEs

$$\begin{aligned} c_2^2(F_1+F_2)F_1' - c_3^2\delta F_1^2 - \gamma c_2^2 F_2^2 - \left[c_3^2\delta + c_2^2(\gamma-\beta)\right]F_1F_2 = 0, \\ c_2^2(F_1+F_2)F_2' + \left(\gamma c_2^2 - c_3^2\delta\right)F_2^2 - \left[c_3^2\delta - c_2^2(\gamma-\beta)\right]F_1F_2 = 0. \end{aligned} \tag{13}$$

The solution of reduced system of ODEs (13) is

$$\begin{aligned} F_1(t) &= \frac{e^{\frac{\left(c_3^2\delta-(\beta-\gamma)c_2^2\right)t}{c_2^2}}A_3\beta - e^{\frac{c_3^2\delta t}{c_2^2}}A_4\gamma}{(e^{-(\beta-\gamma)t}A_3 - A_4)A_4}, \\ F_2(t) &= \frac{e^{\frac{c_3^2\delta t}{c_2^2}}(\gamma-\beta)}{e^{-(\beta-\gamma)t}A_3 - A_4}, \end{aligned} \tag{14}$$

where A_3 and A_4 are arbitrary constants of integration. We substitute the expressions for $F_1(t)$ and $F_2(t)$ from (14) into equation (12). The final form of the group invariant solution of system (1) via combination of Lie symmetries X_2 and X_3 is as follows:

$$\begin{aligned} S(t,x) &= \frac{e^{\frac{c_3(c_3\delta t+c_2x)}{c_2^2}}(e^{-(\beta-\gamma)t}A_3\beta - A_4\gamma)}{(e^{-(\beta-\gamma)t}A_3 - A_4)A_4}, \\ I(t,x) &= \frac{e^{\frac{c_3(c_3\delta t+c_2x)}{c_2^2}}(\gamma-\beta)}{e^{-(\beta-\gamma)t}A_3 - A_4}, \end{aligned} \tag{15}$$

provided $c_2 \neq 0$.

Note that the closed-form solution of the diffusive SIS system (1) provided by (15) corresponds to the closed-form solution via X_2 when we set $c_3 = 0$.

We have considered all possible combinations of Lie symmetries to obtain reductions and closed-form solutions of the diffusive SIS model. For the case when $c_1 \neq 0$, the system of two second-order PDEs (1), representing the diffusive SIS model, reduces to a system of two second-order ODEs. Closed-form solutions are possible when $c_1 = 0$ in the most general symmetry generator. We have established two possible closed-form solutions for this case: one when $c_4 \neq 0$ and the other when $c_4 = 0$. We have explained in detail how the reductions and closed-form solutions for all other possible combinations can be directly deduced from the results presented in this section. This completes the search for the reductions and closed-form solutions of the diffusive SIS epidemic model (1) via Lie symmetry analysis.

3 The Transmission Dynamics of an Influenza Outbreak

In this section, we establish a connection between the closed-form solutions derived in section 2 and a real-world scenario to understand the transmission dynamics of influenza. We consider both the initial conditions and appropriate boundary conditions. Our focus is on addressing the following question: How do varying coefficients of diffusion-both higher and lower-impact the spatiotemporal dynamics of influenza transmission? Moreover, we examine how this insight can contribute to the development of effective strategies to control and mitigate the spread of the disease.

3.1 Initial and boundary conditions

We aim to find expressions for $S(t,x)$ and $I(t,x)$ that satisfy the initial and boundary conditions for $0 \leq x \leq L$ and $0 \leq t \leq T$. The initial conditions are defined as follows

$$\begin{aligned} S(0,x) &= S_0 G(x),\ 0 \leq x \leq L, \\ I(0,x) &= I_0 G(x),\ 0 \leq x \leq L, \end{aligned} \tag{16}$$

where I_0 and S_0 are scaling constants representing the initial densities of susceptible and infected individuals, and $G(x)$ is the initial distributions of susceptible and infected individuals along the domain.

Allen et al [10] utilized the Neumann boundary condition to study the effect of spatial heterogeneity of the environment and individual movement on the extinction and persistence of a disease for SIS epidemic reaction-diffusion models. Huang et al [12] studied a diffusive SIS epidemic model with logistic growth and Dirichlet boundary condition. We consider a homogeneous Neumann boundary condition at $x = 0$ and a time-dependent non-homogeneous Dirichlet boundary condition at $x = L$

$$\begin{aligned}
\frac{\partial S}{\partial x}(t,0) &= 0,\ 0 \le t \le T,\\
\frac{\partial I}{\partial x}(t,0) &= 0,\ 0 \le t \le T,\\
S(t,L) &= H_1(t),\ 0 \le t \le T,\\
I(t,L) &= H_2(t),\ 0 \le t \le T.
\end{aligned} \tag{17}$$

The condition $\frac{\partial S}{\partial x}(t,0) = 0$ ensures that there are no additional incoming susceptible individuals from the outside at the boundary $x = 0$. Similarly, $\frac{\partial I}{\partial x}(t,0) = 0$ indicates no additional incoming infected individuals at the boundary $x = 0$, which aligns with the concept that infected individuals are not entering from outside the modeled region. The conditions $S(t,L) = H_1(t)$ and $I(t,L) = H_2(t)$ allow to specify the behavior of susceptible and infected individuals at the boundary $x = L$ over time. This is important because it allows to model scenarios where interventions, population behaviors, or other factors at the boundary have a time-varying impact on the spread of the disease. For instance, $H_1(t)$ and $H_2(t)$ could represent vaccination campaigns, quarantine measures, or other time-dependent interventions that affect the dynamics of the disease.

We consider the case discussed in subsection 2.2, note that the closed-form solution (11) is defined at the initial time $t = 0$ provided $c_2 > 0$. After straightforward calculations and using the initial conditions (16) and homogeneous Neumann boundary condition at $x = 0$ from (17), we obtain the symmetry constant $c_3 = 0$,

$$F_1(0) = S_0, \quad F_2(0) = I_0, \tag{18}$$

and the following expression for the initial distribution $G(x)$ of susceptible and infected individuals:

$$G(x) = e^{-\frac{c_4}{2c_2}x^2}. \tag{19}$$

It is straightforward to establish the solution of reduced system of ODEs (9) subject to initial conditions (18) and thus the final form of closed-form solution (8) is

$$\begin{aligned}
S(t,x) &= \frac{(I_0+S_0)\sqrt{c_2}}{\sqrt{2c_4\delta t + c_2}} \times e^{\frac{-c_4x^2}{2(2c_4\delta t + c_2)}}\\
&\times \frac{((\gamma-\beta)S_0 + \gamma I_0)\, e^{-(\beta-\gamma)t} - \gamma I_0}{((\gamma-\beta)S_0 + \gamma I_0)\, e^{-(\beta-\gamma)t} - \beta I_0},\\
I(t,x) &= \frac{(I_0+S_0)\sqrt{c_2}}{\sqrt{2c_4\delta t + c_2}} \times e^{\frac{-c_4x^2}{2(2c_4\delta t + c_2)}}\\
&\times \frac{(\gamma-\beta)I_0}{((\gamma-\beta)S_0 + \gamma I_0)\, e^{-(\beta-\gamma)t} - \beta I_0}.
\end{aligned} \tag{20}$$

The closed-form solution (20) is not defined when $\gamma = \beta$. It is worth mentioning that when we take $x = L$ in equation (20), we obtain following

expressions for $H_1(t)$ and $H_2(t)$

$$
\begin{aligned}
H_1(t) &= \frac{(I_0+S_0)\sqrt{c_2}}{\sqrt{2c_4\delta t+c_2}} \times e^{\frac{-c_4L^2}{2(2c_4\delta t+c_2)}} \\
&\times \frac{((\gamma-\beta)S_0+\gamma I_0)\, e^{-(\beta-\gamma)t}-\gamma I_0}{((\gamma-\beta)S_0+\gamma I_0)\, e^{-(\beta-\gamma)t}-\beta I_0}, \\
H_2(t) &= \frac{(I_0+S_0)\sqrt{c_2}}{\sqrt{2c_4\delta t+c_2}} \times e^{\frac{-c_4L^2}{2(2c_4\delta t+c_2)}} \\
&\times \frac{(\gamma-\beta)I_0}{((\gamma-\beta)S_0+\gamma I_0)\, e^{-(\beta-\gamma)t}-\beta I_0}.
\end{aligned}
\tag{21}
$$

and this ensures that the time-dependent non-homogeneous Dirichlet boundary condition at $x = L$ is satisfied.

This completes the closed-form solution of the diffusive SIS model subject to the initial conditions (16) and boundary conditions (17).

3.2 Influenza outbreak

In the context of studying the spread of influenza within a localized community, the diffusive SIS model offers valuable insights into the dynamics of infection transmission. To gain a comprehensive understanding, we explore the closed-form solutions and visualize the initial distribution of susceptible and infected individuals graphically. It is vital to understand the initial spatial distribution of susceptible and infected individuals for control and prevention strategies for influenza outbreak.

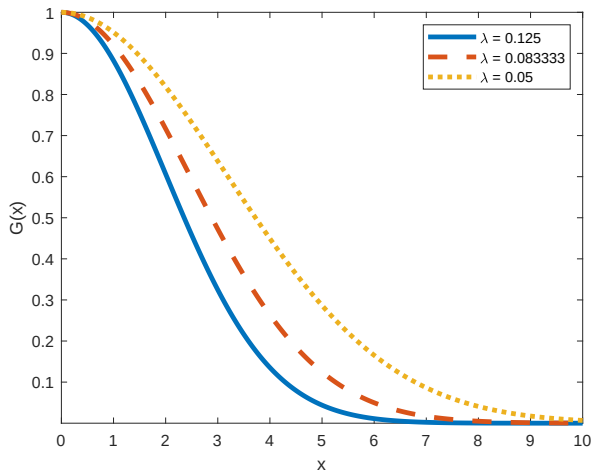

Figure 1: The graphs of initial distribution of susceptible and infected individuals across the domain for different values of $\lambda = \frac{c_4}{2c_2}$ when $0 \leq x \leq 10$.

We can re-write the initial distribution of susceptible and infected individuals $G(x)$ across the domain:

$$G(x) = e^{-\lambda x^2}, \ \lambda = \frac{c_4}{2c_2}. \tag{22}$$

The graphical representation of the initial distribution of susceptible and infected individuals is presented in Figure 1. This graph illustrates the distribution across the domain for different values of the parameter $\lambda = \frac{c_4}{2c_2}$ when $0 \leq x \leq 10$. The parameter $\lambda = \frac{c_4}{2c_2}$ controls the spread and extent of the initial distribution of susceptible and infected individuals along the domain. As λ decreases, the graph expands and spreads out to the right. Thus the smaller values of λ indicate a more spread-out initial distribution. This means that the individuals are more uniformly distributed along the spatial axis.

Now, we examine the closed-form solution for susceptible individuals (S) and infected individuals (I) provided in equation (20), utilizing specific parameter values sourced from existing literature [11, 26, 27]. The following parameter values have been selected: $c_2 = 10$, $c_4 = 1$, $\beta = 0.4$, $\gamma = 0.2$, $S_0 = 10^5 - 200$, and $I_0 = 200$. We consider the spatial range $0 \leq x \leq 10$ and the time interval $0 \leq t \leq 200$ to visualize the closed-form solution (20) graphically.

We consider the lower diffusion coefficient, $\delta = 0.02$, and the higher diffusion coefficient, $\delta = 0.1$, to analyze the effect of diffusion coefficient on the transmission dynamics of influenza outbreak. Figure 2 illustrates the relationship between susceptible individuals $S(x)$ and infected individuals $I(x)$ for fixed values of $t = 20, 30, 50, 70, 200$ for the lower diffusion coefficient $\delta = 0.02$ and higher diffusion coefficient $\delta = 0.1$. Similarly, Figure 3 illustrates the behavior of $S(t)$ and $I(t)$ for fixed value of $x = 0, 2, 4, 6, 10$. The surface plots illustrating the behavior of $S(t, x)$ and $I(t, x)$ are provided in Figure 4. The path of susceptible and infected individuals follow a lower trajectory for higher values of distance, x. This indicates that the density of susceptible and infected individuals decreases with distance from the source of infection. The number of susceptible individuals, S, decreases with time and then stabilizes. The number of infected individuals increases with time, reaches a peak, and then decreases. This pattern reflects an initial rapid spread of infection followed by recovery and susceptibility. Similar dynamics are observed across different locations for both lower and higher diffusion coefficients.

Upon closer examination of figures 2-4, we gain significant observations regarding the behavior of both the infected and susceptible populations which allow us to analyze the effect of the diffusion coefficient on the transmission dynamics of an influenza outbreak. A unique pattern emerges at the boundaries: the source of the disease at $x = 0$ and a distant location at $x = 10$. For the higher diffusion coefficient, $\delta = 0.1$, the reduction in the number of susceptible individuals is more evident at $x = 0$ as time t progresses. In contrast, with a lower diffusion coefficient $\delta = 0.02$, the decline in susceptible individuals at $x = 0$ is less significant over the same time period. Meanwhile, at the boundary $x = 10$, a different trend emerges. As time t progresses, the number of susceptible individuals increases more rapidly when the diffusion coefficient is higher $\delta = 0.1$ compared to when it is lower $\delta = 0.02$. In the rest of spatial domain $0 < x < 10$, as time t approaches $t = 50$, there is a distinct and

sudden decline in the susceptible population, corresponding to the period of rapid infection spread. This decline coincides with the rise in the number of infected individuals, indicating a swift expansion of the influenza outbreak. Beyond $t = 50$, as the number of infected individuals starts to decrease, the susceptible population stabilizes. These trends highlight the accelerated spread of influenza through the population with an elevated diffusion coefficient. Such dynamics in the susceptible population's response emphasize the substantial influence of the diffusion coefficient δ on the course of influenza transmission.

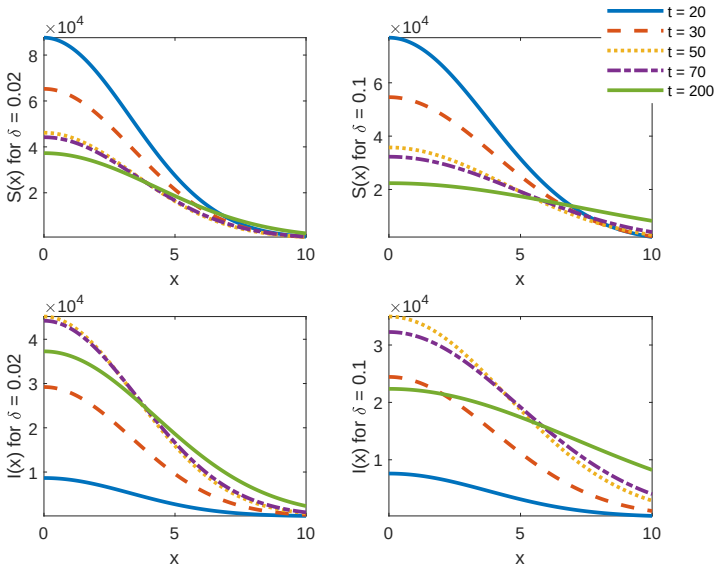

Figure 2: Graphs of $S(x)$ and $I(x)$ for lower ($\delta = 0.02$) and higher ($\delta = 0.1$) diffusion coefficients with $c_2 = 10$, $c_4 = 1$, $\beta = 0.4$, $\gamma = 0.2$, $S_0 = 10^5 - 200$, $I_0 = 200$, over spatial range $0 \leq x \leq 10$.

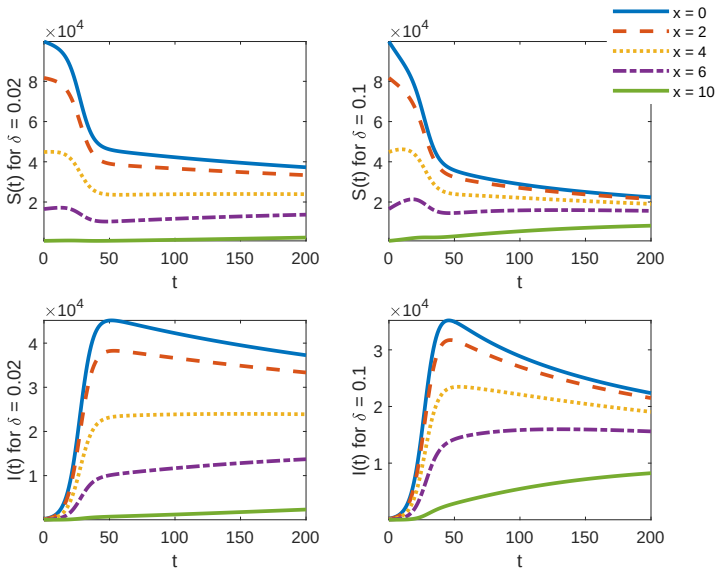

Figure 3: Graphs of $S(t)$ and $I(t)$ for lower ($\delta = 0.02$) and higher ($\delta = 0.1$) diffusion coefficients with $c_2 = 10$, $c_4 = 1$, $\beta = 0.4$, $\gamma = 0.2$, $S_0 = 10^5 - 200$, $I_0 = 200$, over time interval $0 \leq t \leq 200$.

Shifting focus to the infected population, a careful analysis of figures 2-4 reveals that the number of infected individuals increases as time t approaches $t = 50$, subsequently declining as time progresses and same trend is observed across different values of x. Notably, at the boundary $x = 0$, the number of infected individuals is significantly higher for $\delta = 0.02$ than for $\delta = 0.1$. This finding aligns well with our expectations, as a higher diffusion coefficient δ signifies increased mobility, leading to fewer individuals clustering near the boundary $x = 0$. For higher values of both x and t, a noticeable increase in the number of infected individuals is observed when $\delta = 0.1$ than for $\delta = 0.02$. This pattern corresponds to the intuitive understanding that a greater diffusion coefficient expedites the movement of infected individuals, thereby accelerating the propagation of the influenza outbreak.

These insights have important implications for developing efficient public health strategies. The speed at which the influenza spreads is significantly related to diffusion coefficients, as shown by our investigation of how influenza spreads over time and across spatial domain. This indicates that we can specifically target places where the infection is expected to spread more quickly when planning interventions, especially within neighborhood boundaries. We can more effectively distribute resources, such as vaccination programmes, quarantine measures, and medical facilities by identifying these high-risk areas. This will help to limit the outbreak's adverse effects. By considering the specific factors that influence disease

transmission at boundaries, this particular strategy holds great potential as an effective means of managing and containing infectious disease epidemics.

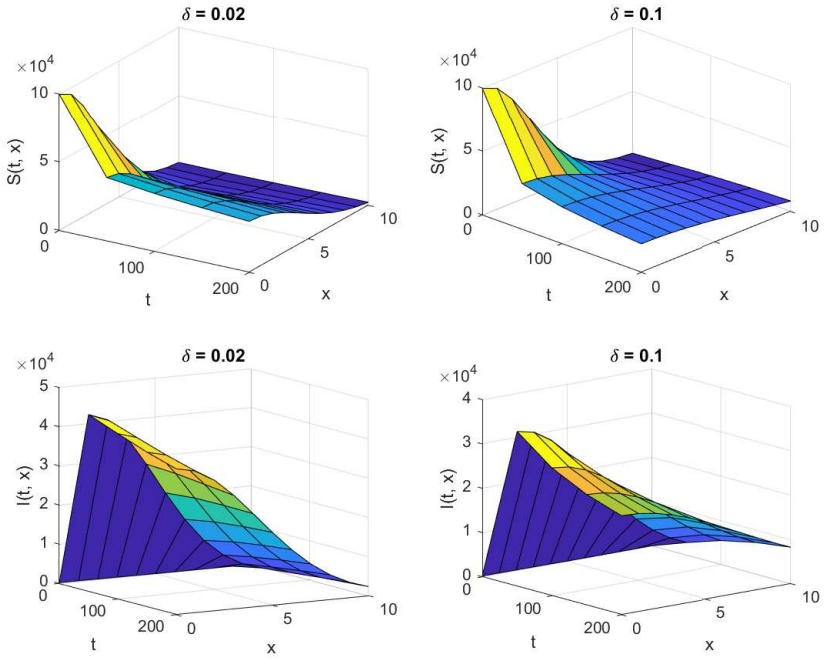

Figure 4: Surface plots of S and I for lower ($\delta = 0.02$) and higher ($\delta = 0.1$) diffusion coefficients with parameters: $c_2 = 10$, $c_4 = 1$, $\beta = 0.4$, $\gamma = 0.2$, $S_0 = 10^5 - 200$, $I_0 = 200$ over time interval $0 \leq t \leq 200$ and spatial range $0 \leq x \leq 10$.

Conclusions

We established the closed-form solutions of the diffusive SIS epidemic model using Lie point symmetries. The model admitted a four-dimensional Lie algebra. We utilized different combinations of Lie symmetries to obtain reductions and closed-form solutions for the diffusive SIS model. The most general Lie symmetry generator led to the reduction of the given system of two second-order PDEs to a system of two second-order ODEs (7). The combination of Lie symmetries X_2, X_3, and X_4 yielded the closed-form solution (11). Another closed-form solution, provided in equation (15), was established by utilizing the combination of Lie symmetries X_2 and X_3. We explained in detail that reductions and closed-form solutions for all other combinations of Lie symmetries can be directly deduced from

these results.

We considered appropriate initial and boundary conditions to explore the biological relevance of these closed-form solutions. We utilized the closed-form solutions to study the transmission dynamics of an influenza outbreak with Gaussian initial distributions. We plotted graphs for the susceptible and infected populations. We considered the lower diffusion coefficient and higher diffusion coefficient to analyze the transmission dynamics of the influenza outbreak.

Funding

This research received no external funding.

Competing Interests

The authors have no relevant financial or non-financial interests to disclose.

Data Availability

Data sharing not applicable to this article as no datasets were generated or analysed during the current study.

References

[1] Cantrell, R. S., & Cosner, C. (2004). Spatial ecology via reaction-diffusion equations. John Wiley & Sons.

[2] Thieme, H. (2006). Book review on Spatial Deterministic Epidemics by L. Rass and J. Radcliffe, AMS, 2003. Math. Biosci, 202, 218-225.

[3] Ruan, S. (2007). Spatial-temporal dynamics in nonlocal epidemiological models. In Mathematics for life science and medicine (pp. 97-122). Springer, Berlin, Heidelberg.

[4] Noble, J. V. (1974). Geographic and temporal development of plagues. Nature, 250(5469), 726-729.

[5] Källén, A. (1984). Thresholds and travelling waves in an epidemic model for rabies. Nonlinear Analysis: Theory, Methods & Applications, 8(8), 851-856.

[6] Källén, A., Arcuri, P., & Murray, J. D. (1985). A simple model for the spatial spread and control of rabies. Journal of theoretical biology, 116(3), 377-393.

[7] Murray, J. D., Stanley, E. A., & Brown, D. L. (1986). On the spatial spread of rabies among foxes. Proceedings of the Royal society of London. Series B. Biological sciences, 229(1255), 111-150.

[8] Murray, J. D., & Seward, W. L. (1992). On the spatial spread of rabies among foxes with immunity. Journal of theoretical biology, 156(3), 327-348. Proceedings of the Royal society of London. Series B. Biological sciences, 229(1255), 111-150.

[9] Shiguesada, N., & Kawasaki, K. (1990). Biological invasions: theory and practice. Oxford series in ecology and evolution.

[10] Allen, L. J., Bolker, B. M., Lou, Y., & Nevai, A. L. (2008). Asymptotic profiles of the steady states for an SIS epidemic reaction-diffusion model. Discrete & Continuous Dynamical Systems, 21(1), 1.

[11] Peng, R., & Liu, S. (2009). Global stability of the steady states of an SIS epidemic reaction-diffusion model. Nonlinear Analysis: Theory, Methods & Applications, 71(1-2), 239-247.

[12] Huang, W., Han, M., & Liu, K. (2010). Dynamics of an SIS reaction-diffusion epidemic model for disease transmission. Mathematical Biosciences & Engineering, 7(1), 51.

[13] Ding, W., Huang, W., & Kansakar, S. (2013). Traveling wave solutions for a diffusive SIS epidemic model. Discrete & Continuous Dynamical Systems-B, 18(5), 1291.

[14] Ovsiannikov, L. V. (1982). Group Analysis of Differential Equations. Academic Press, New York.

[15] Bluman, G. W., & Kumei, S. (1989). Symmetries and Differential Equations. Springer, New York.

[16] Olver, P. J. (1993). Applications of Lie Groups to Differential Equations. Second Edition. Springer Verlag, New York, NY, USA.

[17] Ibragimov, N. H. (Ed.) (1994-1996). CRC Handbook of Lie Group Analysis of Differential Equations. vols. 1-3, CRC Press, Boca Raton, FL.

[18] Champagne, B., Hereman, W., & Winternitz, P. (1991). The computer calculation of Lie point symmetries of large systems of differential equations. Computer Physics Communications, 66(2-3), 319-340.

[19] Hereman, W. (1993). SYMMGRP. MAX and other symbolic programs for lie symmetry analysis of partial differential equation. Lectures in Appl. Math, 29, 241-257.

[20] Hereman, W. (1996). Symbolic software for Lie symmetry analysis. CRC Handbook of Lie group analysis of differential equations, 3, 367-413.

[21] Cheviakov, A. F. (2007). GeM software package for computation of symmetries and conservation laws of differential equations. Computer physics communications, 176(1), 48-61.

[22] Rocha Filho, T. M., & Figueiredo, A. (2011). [SADE] a Maple package for the symmetry analysis of differential equations. Computer Physics Communications, 182(2), 467-476.

[23] Hereman, W. (1997). Review of symbolic software for Lie symmetry analysis. Mathematical and Computer Modelling, 25(8-9), 115-132.

[24] Haq, B. U., & Naeem, I. (2019). First integrals and exact solutions of some compartmental disease models. Zeitschrift für Naturforschung A, 74(4), 293-304.

[25] Haq, B. U., & Naeem, I. (2019). First integrals and analytical solutions of some dynamical systems. Nonlinear Dynamics, 95(3), 1747-1765.

[26] Naz, R., & Al-Raeei, M. (2021). Analysis of transmission dynamics of COVID-19 via closed-form solutions of a susceptible-infectious-quarantined-diseased model with a quarantine-adjusted incidence function. Mathematical Methods in the Applied Sciences, 44(14), 11196-11210.

[27] Samsuzzoha, M., Singh, M., & Lucy, D. (2011). Numerical study of a diffusive epidemic model of influenza with variable transmission coefficient. Applied Mathematical Modelling, 35(12), 5507-5523.